INTEGRATING SATELLITE REMOTE SENSING AND GIS FOR ANALYSING URBAN HEAT ISLAND

Wan Mohd Naim Wan Mohd[1], Suhaila Hashim[2] and Abdul Malek Mohd Noor [3]

[1,2,3]Faculty of Architecture, Planning and Surveying , Universiti Teknologi MARA, Shah Alam, MALAYSIA

ABSTRACT

Urban Heat Island is a reflection of microclimate changes brought about by the man-made alterations to the urban surfaces. Recent studies have indicated that satellite remote sensing and Geographical Information System (GIS) technologies inherently suited for studies related to land use/land cover changes, environmental assessment and monitoring, geology, hydrology and various other applications. The objectives of this study are to determine the i) relationship between spectral reflectance of thermal infrared (IR) band of Landsat image and urban surface temperature ii) relationship between surface temperature and land use/land cover types and iii) effect of vegetation on the surrounding surface temperature. An area which covers the Petaling and Klang districts has been selected as the study area. Landsat 7 Enhance Thematic Mapper Plus (ETM+) image of 15th of July 2000 is used in the study. Surface temperature maps and land use/land cover maps are generated from the satellite image. For a more detailed study on the effect of the surrounding vegetation and building properties, scanned aerial photo, and SPOT 5 satellite images are used as image backdrop. Findings from this research have shown that there is a strong correlation between the digital number of the thermal infrared band of Landsat satellite image. The temperature derived from the models obtained from this research is almost similar to that of other established models such as Markham and Barker's Model, Quadratic Regression Model, and Cubic Regression Model. Temperature maps derived from satellite images have shown the differences in surface temperature for different land use, with forested or green areas and industrial areas exhibit the lowest and highest temperature respectively. The effect of vegetation on the surrounding surface temperature is clearly evident in this study.

Introduction

The process of urbanization has created the urban heat island. As a city expands, trees are cut down to accommodate commercial development, industrial areas, roads, and suburban growth. Trees or green areas normally reduce the amount of heat and smog generated by populated areas. Plants and water-retaining soils absorb heat during the day, and then carry the heat away through evaporation. Earlier studies by Oak (1987) and Lowry (1977) have identified micro topography, weather condition, city roughness, city density, city pattern, urban activity and thermal characteristics of the city surface as major factors which influence urban climate. Studies by Carlson *et al.* (1981), Lo *et al*., (1997) and Owen (1998) have identified that UHI are the result of the replacement of pre-existing natural landscapes (principally natural vegetation) by heat absorbing surfaces such as building roofs, walls, parking lots and streets.

Due to this, there is a serious concern nowadays on quantifying surface temperature in urban areas and investigating UHI mitigation measures in terms of reduced energy use and air pollution. Through the implementation of measures designed to mitigate the urban heat island (mainly related to deforestation and use of highly reflective building and pavement surfaces), communities could decrease their demand for energy and/or effectively "cool" the urban landscape (Taha *et al*., 1997 and Chen *et al*., 2001).

Many of the earlier studies investigated the issues of the relative warmth of cities by measuring the air temperature employing land-based observations of weather stations. Other studies used scheduled measurements of temperature using temperature sensors mounted on a

ISSN 1675-5022

car, along various routes (Yamashita, 1996; Comire, 2000; Pinho and Manso, 2000). These methods can be both costly and restricted in coverage. Observations of remotely sensed UHI using aircraft and satellite-based systems exhibit different features from those measured from air temperature directly and their interpretation is often difficult (Price, 1979 and Vukovich, 1983). Recent studies by Rao (1972), Matson *et al.* (1978), Price (1979), Carlson *et al.* (1981), Lo *et al*., (1997) and Owen (1998) have indicated that satellite remote sensing is one of the promising technologies inherently suited for understanding the relationship between land cover change and changes in surface temperature. The advantage of using remote sensing data is contingent on the availability of high resolution, consistent and repetitive measurements of earth surface conditions (Owen *et al.*, 1998).

Rao (1972) was the first researcher to demonstrate that surface temperature of urban areas could be identified by analysing thermal infrared (IR) data acquired from satellite. Matson *et al.* (1978) utilised Very High Resolution Radiometer (VHRR) thermal IR data (with spectral reflectance of 10.5 – 12.5μm) acquired at night to examine urban and rural surface temperature differences. Price (1979) utilised Heat Capacity Mapping Mission (HCMM) data (also with spectral reflectance of 10.5 – 12.5 μm) to assess the extent and intensity of urban surface heating in the northeastern United States.

It is well known that remote sensing technology can be used to monitor land cover and the climatic environment of the earth's surface. It is possible to use this technology to investigate the interaction between land cover and local climate. Thermal remote sensing of satellite and airborne-based sensors are acceptable techniques for global, regional and local observations. National Oceanic and Atmospheric Administration Advanced Very High Resolution Radiometer (NOAA AVHRR) imagery with spatial resolution of 1.1 km have been used by several researchers for example Gallo *et al.*, (1993), Franca and Cracknell (1994), Reutter *et al*., (1994) to derive surface temperature at global and regional scales. Examples on the use of Landsat satellite (Landsat Thematic Mapper (TM) Landsat 7 ETM+) thermal data for urban heat island can be found in Chen *et al.,* (2001), Jo *et al*. (2000), Suga *et al.*, (2000), Kim (1992) and Roth *et al*. (1989). The spatial resolutions for the thermal bands for Landsat TM and Landsat ETM+ are 120 and 60m respectively. The much improved spatial resolution on the thermal band of the Landsat ETM+ as compared to the Landsat TM and NOAA-AVHRR makes a more detailed analysis of the urban microclimate possible. Due to its superior spatial resolution, airborne imagery with spatial resolution of less than 10 metres are being used in many earlier urban heat island study (e.g. Lo *et al*., 1997, Quattrochi and Lavall, 1997).

Over the years a number of models have been developed by different authors (Markham and Barker, 1986; Aniello *et al.*, (1995), Chen *et al*., (2001), Jo *et al.*, 2001) to convert satellite data into surface temperature. Procedure to derive the surface temperature as used in Chen *et al.* (2001) requires three-step; i) conversion of Digital Number (DN) to spectral radiance ii) conversion of the spectral radiance to temperature and iii) Emissivity Correction. Jo *et al.,* (2001) in his study used four (4) different models i.e. two point linear model, linear regression model, quadratic regression model and cubic regression model. These models are as follows:

Two-point linear model

$$Temp(°K) = 203.2 + 0.541176 \times TM6 \quad \text{......[1]}$$

Linear regression model

$$Temp(°K) = 219.97218 + 0.525959 \times TM6 \quad \text{......[2]}$$

Quadratic regression model

$$Temp(°K) = 209.830966 + 0.834313 \times TM6 - 0.001372 \times TM6^2 \quad \text{......[3]}$$

Cubic regression model

$$Temp(°K) = 206.127 + 1.054 \times TM6 - 0.003714 \times TM6^2 + 6.60655 \times 10\text{-}6 \times TM6^3 \quad \text{......[4]}$$

where
Temp(°K) - absolute temperature
TM6 – digital number of thermal IR band

Study Area And Material Used

The study area of this research covers the Petaling and Klang districts. This area has been selected as study area because the existence of diverse land use including residential, industrial, commercial, cleared land, forest, water bodies and the availability of Landsat images. The study area covers an area of 40 km (East-West) by 33 km (North-South). In this study, Landsat 7 ETM+ image of 15th of July 2000 acquired from the Malaysian Centre for Remote Sensing (MACRES) and temperature data of eight (8) Continuous Air Quality Monitoring (CAQM) Stations were used. Landsat 7 was launched on the 15th of April 1999 with ETM+ sensor and a multi-spectral scanner with eight (8) bands (visible bands :- Band 1: 0.45 – 0. 52 μm, Band 2: 0.53 – 0.60μm and Band 3: 0.63 – 0.69μm; near-infrared bands :- Band 4: 0.76 – 0.90 μm; short-wave infrared band – Band 5: 1.55 – 1.75μm and Band 7: 2.09 – 2.35μm; thermal band – Band 6: 10.4 – 12.5μm) and the panchromatic band – Band 8: 0.52 – 0.90μm). The spatial resolution of the panchromatic and thermal IR bands are 15 and 60 metres respectively. Figure 1 shows the LANDSAT 7 ETM+ colour composite images (Band 4 : red, Band 3 : green and Band 2 : blue) of the study area. Scanned aerial photographs and SPOT 5 satellite image were also used as image backdrop. Figure 2 shows the thermal IR image of the study area. Rectified aerial photo of part of the study area and SPOT 5 Panchromatic images are given in figures 3 and 4 respectively.

Hourly temperature data of the meteorological observation stations acquired from the Meteorological Services Department of Malaysia are used to determine the relationship between Landsat image digital number or spectral reflectance of the thermal IR band and surface temperature. The station location and ground temperature at these stations are given in Table 1.

Table 1: Location of observation stations and ground temperature

Stn ID	CAQM Station	**Eastings (m)**	**Northings (m)**	**Temp (^{o}C)**
1	Kuala Lumpur	347259.642	412068.035	29.1
2	Gombak	360939.767	406228.961	26.8
3	Kajang	331326.620	416100.169	26.4
4	Klang	333215.041	379076.943	28.8
5	Petaling Jaya	344174.824	412060.761	27.9
6	Shah Alam	340586.252	390560.750	28.7
7	Nilai	312145.011	424221.805	26.3
8	Seremban	301369.706	441298.924	27.3

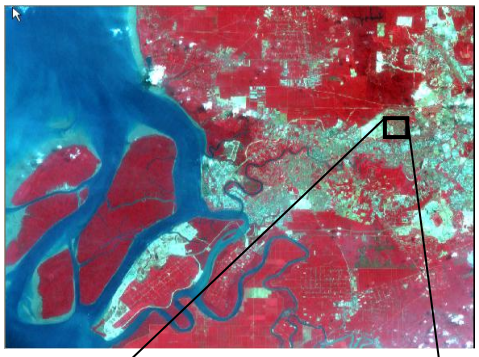

Figure 1: Landsat 7 ETM+ image of the study area

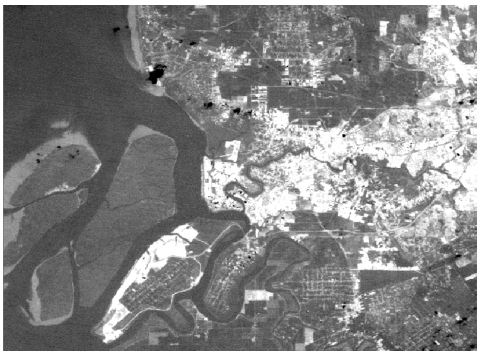

Figure 2: Thermal image (band 6) of the study area

Figure 3: Rectified aerial photo image of part of the study area

Figure 4: SPOT 5 Panchromatic image of the study area

Methodology

The overall research methodology adopted for this research is given in Figure 5. Based on the thermal IR image and the surface temperature of the CAQM stations located within the Klang Valley Region and Negeri Sembilan, regression analysis is carried out to determine the relationship between Landsat DN and surface temperature. Two different regression equations i.e. linear and quadratic regression were tested. Different CAQM station configurations were used i.e. 8, 7, 6, 5 and 4 stations. The eight (8) station configuration includes the Nilai and Seremban CAQM stations. Beside regression analysis, the derived equations were compared to the results obtained from other well established models i.e. Two-point Linear model, Linear Regression model, Quadratic Regression model, Cubic regression model and Markham and Barker's model.

From the geometrically corrected Landsat 7 ETM+ image, unsupervised image classification is carried out and the land use/land cover are classified into a number of categories. Thermal band if the Landsat 7 ETM+ image was used to derive the surface temperature map. Scanned aerial image is rectified using coordinates of Ground Control Points (GCPs) derived from Global Positioning System (GPS). The process of image rectification, and image classification is carried out in the ERDAS Imagine digital image processing software. Thermal IR band from the ERDAS Imagine software is directly transferred and read in ArcGIS software. The thermal IR images are converted into surface temperature maps using the derived model in the GIS software.

To determine the relationship between surface temperature and land use/land cover temperature at thirty well defined locations of the same feature categories (e.g. residential, industrial, water bodies, forest and cleared land) are measured from temperature maps of the study area. Mean temperature of each feature categories is then calculated. To analyse the effect of different vegetations, buildings and roads, temperature of fifteen (15) points (five

for each feature) which are located on roads, within open space and residential areas are extracted. A 100 m buffer is drawn from the identified points and the percentage of vegetation coverage, building density and road density are manually measured and later compared to surface temperature. The overall methodology adopted for this study is given in Figure 5.

Results And Analysis

Relationship between spectral reflectance of thermal infrared (IR) band of Landsat images and urban surface temperature

Table 1 summarise the linear regression equations obtained from the correlation between DN of the thermal IR band of Landsat ETM+ and ground surface temperature of three different dates. The summary on quadratic regression equations obtained for the image acquired on the 15th of July 2000 is given in Table 2. The R^2 coefficients using 8, 7, 6, 5 and CAQM stations are 0.6119, 0.7847, 0.9287, 0.9495 and 0.8852 respectively. Using quadratic regression equations, the R^2 coefficients using 8, 7 and 6 CAQM stations are 0.792, 0.8410 and 0.9365 respectively.

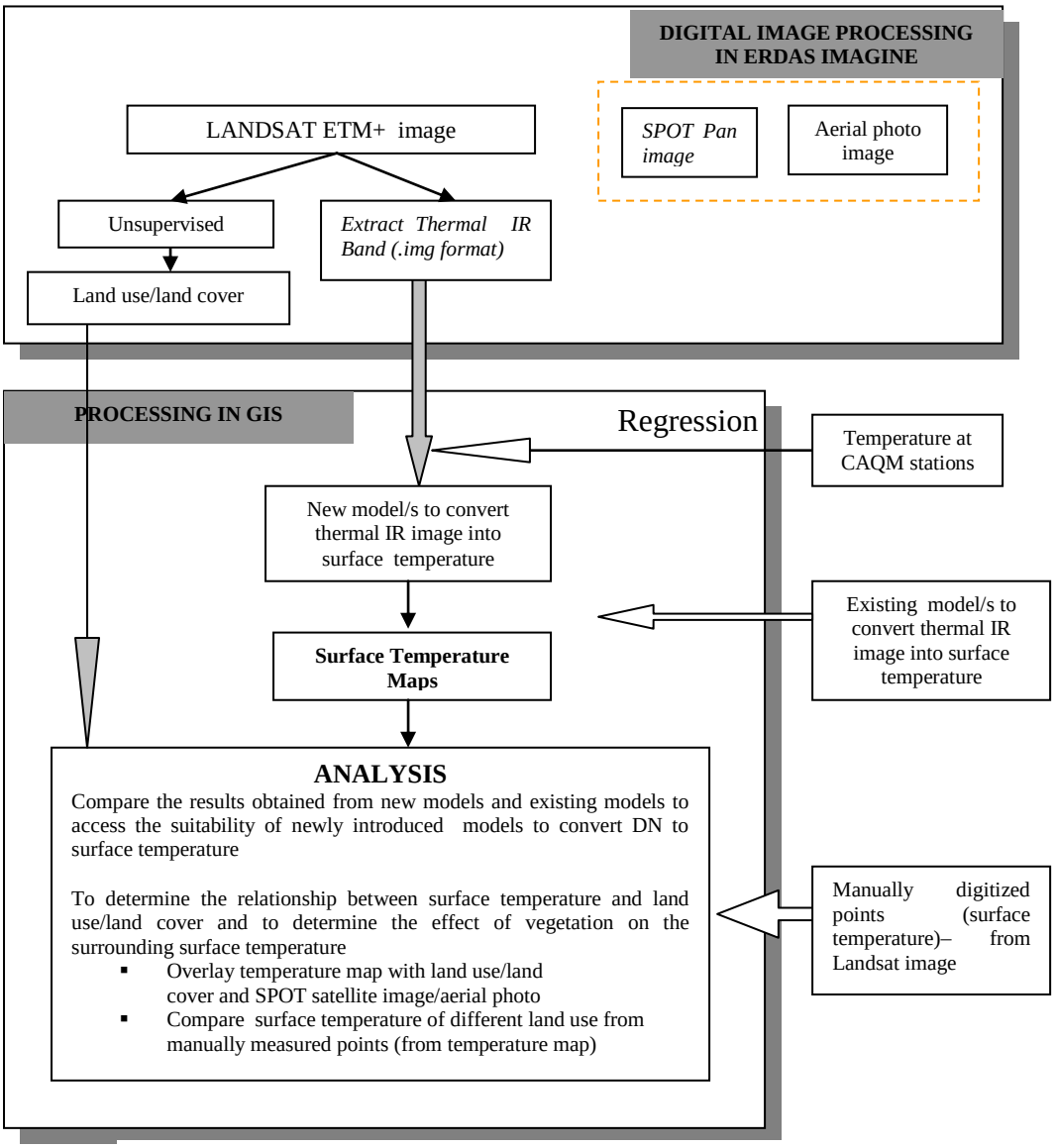

Figure 5 : Steps of analysis and comparison between urban heat island and land use/land cover

Table 2: Linear regression equations between DN (thermal infrared band) of Landsat 7 ETM+ image and surface temperature

No. of CAQM station	Linear Regression Equation	R^2
8	Y = 1.9456x + 92.316	0.6119
7	Y = 1.7851x + 97.253	0.7847
6	Y = 2.2463x + 84.066	0.9287
5	Y = 2.4661x + 77.72	0.9495
4	Y = 3.2685x + 54.687	0.8852

Table 3: Quadratic regression equations between DN (thermal infrared band) of Landsat 7 ETM+ image and surface temperature

No. of CAQM station	Quadatic Regression Equation	R^2
8	$Y = 1.5734x^2 – 85.116x +1295$	0.7920
7	$Y = 0.8304x^2$ -44.127+730.83	0.8410
6	$Y = 0.3362x^2 – 16.391x + 341.97$	0.9365

Note: Y – Spectral Reflectance of thermal infrared band or digital number
x – Surface temperature

Based on the regression models given in tables 2 and 3 only five models with high correlation coefficients (R^2) were selected. The five models are as follows:

Y = 2.2463x + 84.066 (R^2 = 0.9287) New Model 1 (NM1)
Y = 2.4661x + 77.72 (R^2 = 0.9495 New Model 2 (NM2)
Y = 1.5734x2 – 85.116x +1295 (R^2 = 0.7920) New Model 3 (NM3)
Y = 0.8304x2 -44.127+730.83 (R^2 = 0.8410) New Model 4 (NM4)
Y = 0.8304x2 -44.127+730.83 (R^2 = 0.9365) New Model 5 (NM5)

Figure 6 graphically shows the differences in surface temperature obtained from different models. Results clearly show the higher the satellite DN the higher the surface temperature (positive correlation). The two-point linear (TPM) model as developed by Jo *et al.*, (2000) is not suitable to be used to calculate ground surface temperature as it gives a much lower temperature as compared to other models. Linear regression model is also not suitable to calculate surface temperature from lower satellite DN (i.e. DN lower than 133). The surface temperature obtained from New Model 1 (NM1) and New Model 2 (NM2) as proposed by the author is quite similar to that of the Cubic regression model (used by Jo *et al.*, 2000) and the well established Markham and Barker's model.

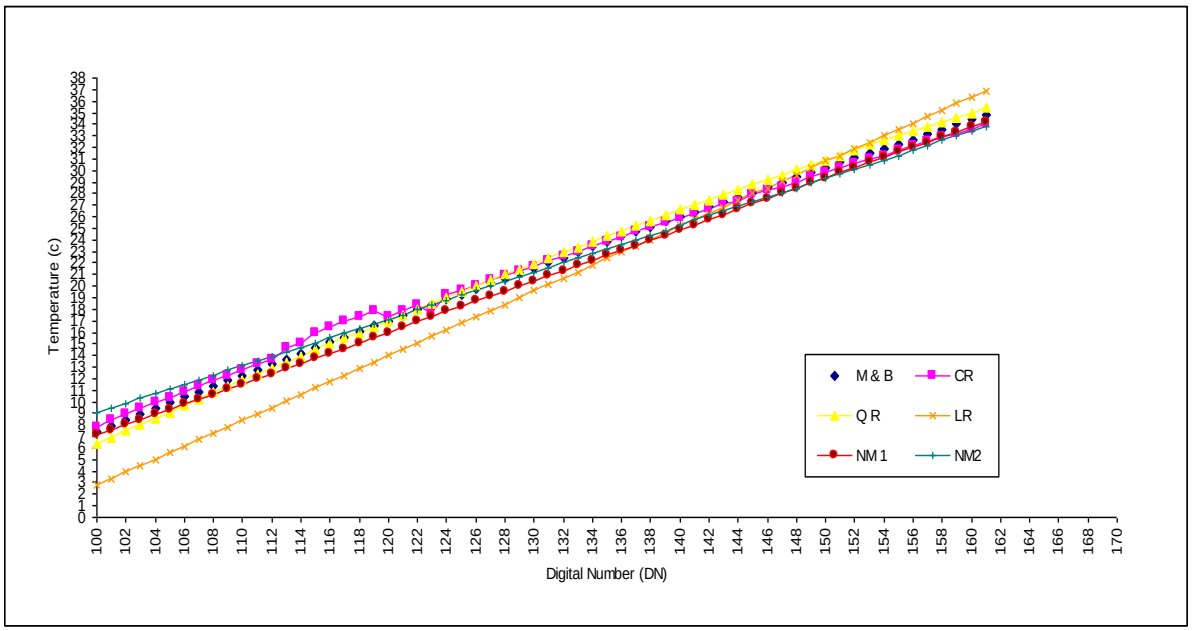

Figure 6: Derived Surface Temperature (C) against Satellite DN using various models

Relationship Between Land Use/Land Cover And Ground Surface Temperature

Results of this study have shown that the maximum difference in the surface temperature of different land cover types is almost 14^{o}C. The minimum and maximum surface temperature are 22.95 and 36.2^{o}C respectively. The mean surface temperature of land use/land cover (as shown in Figure 7) range from 23.4 to 33.6 ^{o}C (approximately 10 ^{o}C). The temperature of various land use/land cover types range from high to low are as follows: industrial, residential/commercial, cleared land, water bodies, green areas and forest. This result indicates a strong relationship between different land use/land cover types and surface temperature. Figures 8 a) and 8 b) show the land use/land cover map and surface temperature map of the study area. In the Kelang District, especially the western part of Pulau Indah and the town areas, the surface temperature is much higher than the surrounding areas. In the Shah Alam, high temperature zones are located in sections 15, 16, and 24.

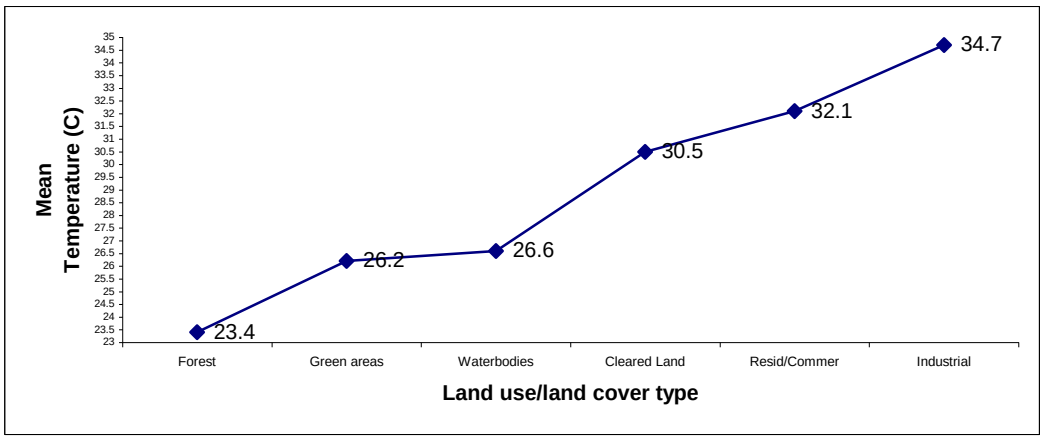

Figure 7: Mean surface temperature of different land use/land cover types

To analyse and visualise the relationship between surface temperature and land use/land cover types, merged colour maps are produced. In Figure 9 a), the surface temperature map is overlaid onto a SPOT panchromatic image. For a more detailed analysis on the influence of

land use/land cover types on the surface temperature, the surface temperature map is overlaid onto rectified aerial photo image of a small part of the study area (University Teknologi MARA campus). Figure 9 b) shows that the industrial areas which is shown in dark brown and red colours exhibit the highest temperature. This could be due to aluminum roof material. The effect of vegetation in a neighbourhood is clearly evident in Figure 9 b) (area indicated in the red box). Vegetation reduces the ambient temperature by evapotranspiration.

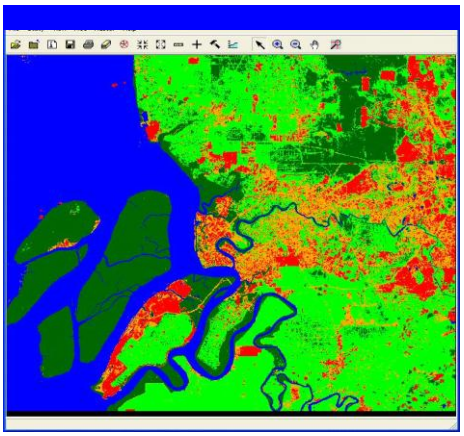

Figure 8 a): Land use/land cover surface temperature map of the study

Figure 8 b): Surface temperature map of the study area

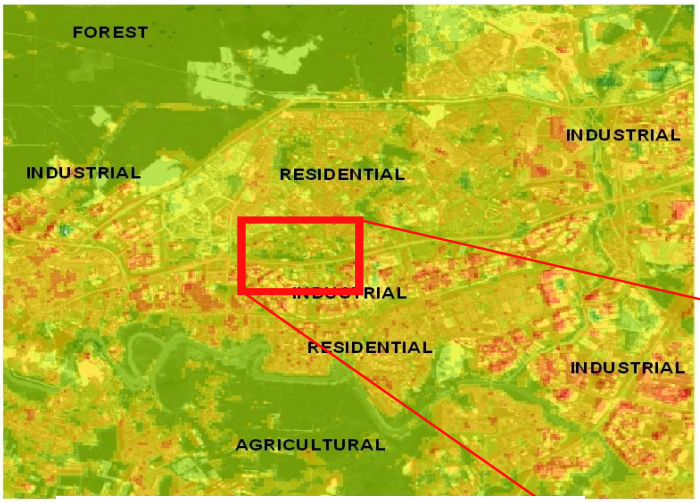

Figure 9 a): Surface temperature map overlaid onto SPOT panchromatic image

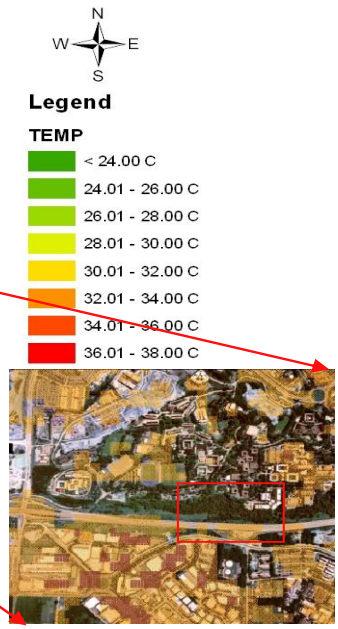

Figure 9 b): Surface temperature map overlaid onto aerial photo image

Effect Of Vegetation On The Ground Surface Temperature

Temperature of fifteen (15) points extracted from the generated surface temperature maps (from Landsat images year 2000) of three different features i.e. residential areas, roads and open space are summarised in Table 4. Results presented in this table have shown that the presence of trees within 100 metres of the feature significantly reduce the surface temperature of the area. Figure 10 shows the locations of the selected points.

Table 4: Surface temperature of residential, road surface and open space

Residential Area/ID	Trees (%)	Buildings (%)	Road (%)	Temp (°C) - 2000	Temp (°C) - 2001
R 1	10	70	20	30.6	30.2
R 2	35	50	15	28.3	27.1
R 3	40	55	5	29.8	27.1
R 4	35	55	10	29.8	28.6
R 5	5	65	30	29.8	30.6
Road/ID	Trees (%)	Buildings (%)	Road (%)	Temp (°C) - 2000	Temp (°C) - 2001
Rd 1	10	60	30	32.1	30.2
Rd 2	60	-	40	28.3	29.4
Rd 3	5	80	15	30.6	30.6
Rd 4	70	20	10	28.6	28.3
Rd 5	30	40	30	30.6	30.6
Open Space/ID	Trees (%)	Buildings (%)	Road (%)	Temp (°C) - 2000	Temp (°C) - 2001
OP 1	60	10	30	29.0	30.2
OP 2	70	-	30	27.1	29.0
OP 3	30	10	60	31.3	31.7
OP 4	80	20	-	29.0	29.0
OP 5	65	30	5	29.0	27.1

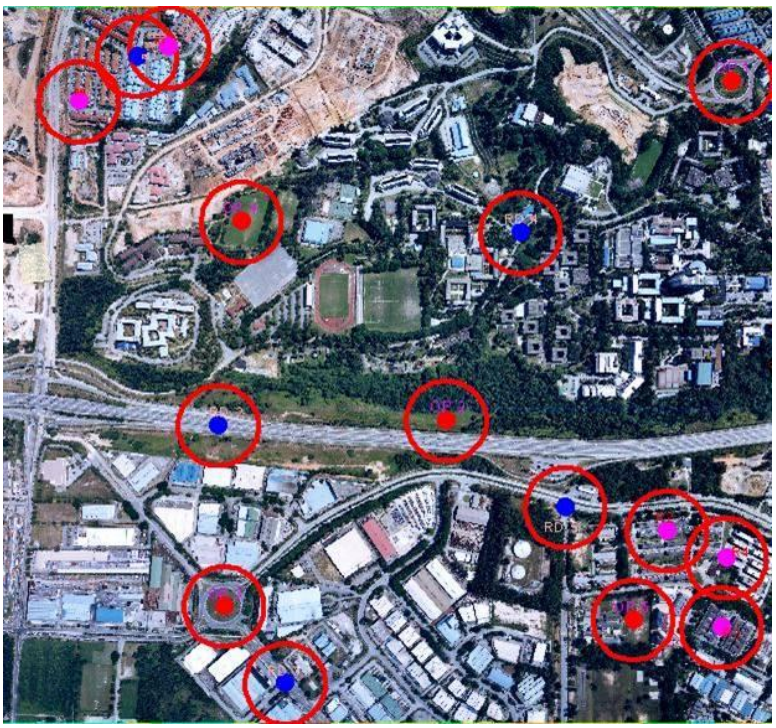

Figure 10: Locations of the selected features

Conclusions And Recommendations

Although this initial study is not comprehensive, the findings from this research can be summarised as follows:-

- satellite-based image provide a low-cost means of deriving surface temperature and time-synchronous coverage of the study area
- it gives an insight in the urban heat island phenomena of an urban area
- there is a strong relationship between land use/land cover types with surface temperature
- green areas or trees within an urban area will significantly reduce the surface temperature.

Results from this study can be used by urban planners to plan appropriate strategies to minimize the effect of urban heat island within the Malaysian cities. Future studies should explore the potential use of other high resolution sensors especially airborne hyperspectral images to analyse urban heat island.

Acknowledgements

The authors express their sincere gratitude to the Institute of Research, Development and Commercialisation (IRDC) UiTM for providing the grant to carry out this research, the Malaysian Center for Remote Sensing (MACRES) for providing LANDSAT and SPOT images of the study area and also the assistance of Hj Desa b. Ali.

References

Balling, R. and Brazel S. W., 1988. High resolution surface temperature patterns in a complex urban terrain. *Photogrammetry Engineering and Remote Sensing*. 54, 1289 – 1293.

Carlson, T. N., Augustine J. N. and Boland F. E., 1977. Potential application of satellite temperature measurements in analysis of land use over urban areas. *Bulletin of the American Meteorological Society.* 58, 1301 – 1303.

Carlson, T.N., Dodd, J.K., Benjamin S. G., and Cooper, J.M., 1981. Satellite estimation of the surface energy balance, moisture availability and thermal inertia. Journal of Applied Meteorology, 20, 67 – 87.

Chen *et al.*, (2001), Chen, P., S. C. Liew and L. K. Kwoh, 2001. Dependence of Urban Temperature Elevation on Land Cover Type. *22nd Asian Conference on Remote Sensing*.

Comire, A., 2000. Mapping a wind-modified urban heat island in Tucson, Arizona (with comments on Integrating Research and Undergraduate Learning). Bulletin of the American Meteorological Society, Vol. 18, No. 10, 2417 - 2413.

Franca, G. B. and Cracknell A. P, 1994. Retrieval of land and sea surface temperature using NOAA-11 AVHRR data in North-eastern Brazil. *International Journal of Remote Sensing,* 15, 1695-1712.

Gallo, K.P., A.L. Mc Nab, T.R. Karl, J.C. Brown, J. J. Hood and J. D. Tarpley, 1993. The use of a vegetation index for assessment of the urban heat island effect. Volume 14 in *International Journal Remote Sensing.* 11, 2223 – 2230.

Jo M H., J.,L. Kwang, J. H. Shin, H. S. Suh, S. N. Oh, 2000. Surface Temperature Analysis of Urban Area Using RS and GIS. Department of Geodetic Engineering, Kyungil University.

Kim, H. H., 1992. Urban Heat Island, Volume 13 in *International Journal Remote Sensing.* 12, 2319 – 2336.

Lillesand, T.M. and Kiefer, R.W., 1994. Remote Sensing and Image Interpretation, Wiley, New York pp 529 - 597.

Lo, C.P., D.A. Quattrochi, J. C. Luvall, 1997. The Urban Heat Island Effect. *International Journal Remote Sensing.*

Markham, B. L and J. K. Baker, 1986. LANDSAT MSS and TM post-calibration dynamics ranges, atmospheric reflectance and at-satellite temperatures, *EOSAT LANDSAT Technical Notes. No. 1 EOSAT*, Lanham, Maryland.

Matson, M., E.P. Mc Clain, D.F. Mc Ginnis, Jr., and J.A. Pritchard, 1978. Satellite detection of urban heat islands. Monthly. Weather. Rev., 106, 1725 – 1734.

Nicol, J. E, 1994. A GIS-based approach to microclimate monitoring in Singapore high-rise housing estate. *Photogrammetric Engineering and Remote Sensing.*

Ozawa A., B.B Madhavan, H. Okada, K.K. Mishra, K. Tachibana and T. Sasagawa, 2004. Airborne Hyperspectral and Thermal Information for Assessing The Heat Island in Urban Areas of Japan **XXth** ISPRS Congress, 12-23 July 2004 Istanbul, Turkey

Pinho and Manso, 2000). Price, J. C., 1991. Timing of NOAA afternoon passes. International Journal of Remote Sensing, 12, 193 – 198.

Price, J. C., 1991. Timing of NOAA afternoon passes. International Journal of Remote Sensing, 12, 193 – 198.

Price, J.C., 1979. Assessment of the urban heat island effect through the use of satellite data. Monthly Weather Review, 107, 1554 – 1557.

Quattrochi, D. A. and J.C. Luvall, 1997. High Spatial Resolution Airborne Multispectral Thermal Infrared Data to Support Analysis and Modelling Task in EOS IDS Project Atlanta. NASA, Global Hydrology and Climate Center, Huntsville, AL. Http://wwwghcc.msfc.nasa.gov.atlanta.

Quattrochi, D. A. and J.C. Luvall, 1997. High Spatial Resolution Airborne Multispectral Thermal Infrared Data to Support Analysis and Modelling Task in EOS IDS Project Atlanta. NASA, Global Hydrology and Climate Center, Huntsville, AL. Http://wwwghcc.msfc.nasa.gov.atlanta.

Rao, P.K., 1972. Remote Sensing of urban heat islands from an environmental satellite. Bull. Amer. Meteor. Soc., 53, 647 - 648.

Reutter, H., Olesen F. S. and Fisher H., 1994. Distribution of the brightness temperature of land surface determined from AVHRR data. *International Journal of Remote Sensing.* 15, 95 – 104.

Rohinton, M.E., 2001. Summertime Heat Islands Effects of Urban Design Parameters. Http://www.umich.edu.

Roth, M., Oak T.R. and Emery W. J., 1989. Satellite derived Urban Heat Islands from three coastal cities and the utilization of such data in urban climatology. *International Journal of Remote Sensing* 10, 699 – 720.

Suga, Y., M. Yoshimura, S. Takeuchi and Y. Oguro. Verification of Surface Temperature from Landsat 7/Etm+ Data. *21th Asian Conference on Remote Sensing.*

Yamashita, S., 1996. Detailed structure of heat island phenomena from moving observations from electric trans-cars in Metropolitan Tokyo. Atmospheric Environment, Vol. 30, 429 - 435.